Supplementary Information

Figure 1

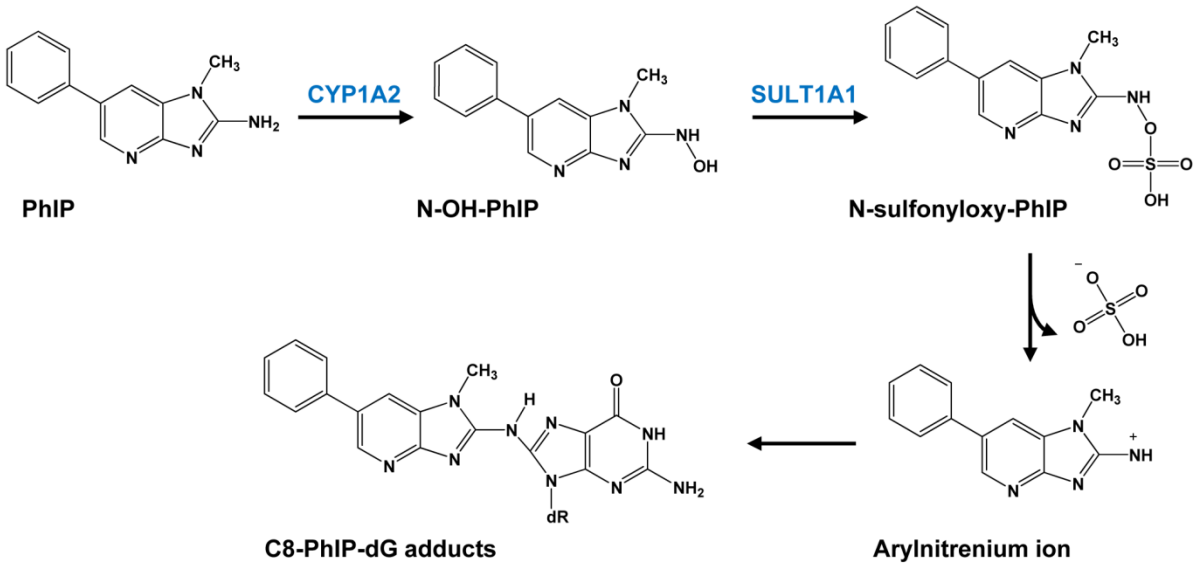

Figure 1: Metabolism of PhIP and DNA adduct formation. PhIP is activated by CYP1A2 in the liver, resulting in the generation of N-OH-PhIP. This toxic metabolite is conjugated with sulphate in a reaction catalysed by SULT1A1. Alternatively, N-OH-PhIP can undergo acetylation by NATs (not shown). The formed N-sulfonyloxy-PhIP is then transported via the bloodstream to the distal colon, where it is actively secreted from the colon mucosa into the lumen, thereby passing through the stem cell compartment in the colon crypts. Due to its instability, a DNA-reactive arylnitrenium ion is released, which reacts with DNA, thereby yielding primarily C8-PhIP-dG adducts.

Figure 2

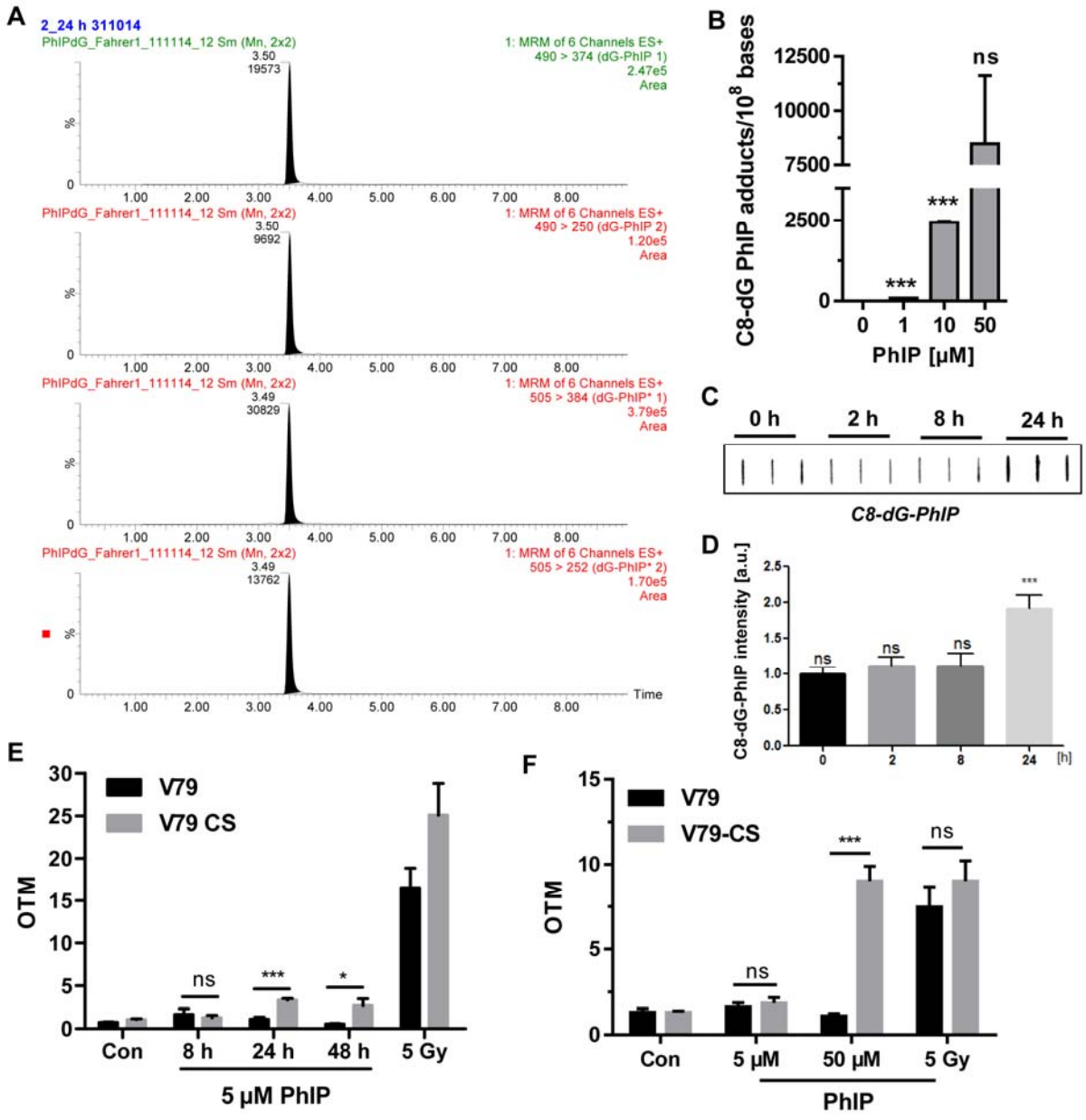

Figure 2: Determination of C8-PhIP-dG adducts and induction of DNA strand breaks. (A) UPLC-MS/MS chromatograms of a digested DNA sample from CYP1A2/SULT1A1-expressing V79 cells incubated with PhIP. The chromatograms of C8-PhIP-dG (m/z = 490.1 → 374.1 and m/z = 490.1 → 250.1) (upper panels) are shown together with the parallel recording of [$^{15}N_5$,$^{13}C_{10}$]C8-PhIP-dG fragmentational chromatograms (m/z = 505.1 → 384.1 and m/z = 505.1 → 252.1) (lower panels). **(B)** Dose-dependent induction of C8-PhIP-dG DNA adducts. V79 CS cells were incubated with increasing concentrations of PhIP (0 – 50 µM) for 24 h. Genomic DNA was isolated and analyzed for C8-PhIP-dG adducts by mass spectrometry using an isotope-labeled reference standard. Data are presented as mean + SEM (n=3 per dose); ***p<0.001, ns not significant. **(C)** Detection of PhIP DNA adducts in

genomic DNA isolated from V79 CS cells following incubation with 50 µM PhIP for up to 24 h. Samples (triplicates, 500 ng per slot) were subjected to immunological slot blot analysis as described under material and methods. A representative dot blot is shown. **(D)** Densitometric evaluation of PhIP DNA adduct analysis from two independent experiments with triplicates each **(E)** Parental V79 and V79 CS cells were challenged with 5 µM PhIP for up to 48 h. As a positive control, cells were irradiated with 5 Gy. Cells were harvested and analyzed by performing the alkaline Comet-Assay. Data are expressed as mean + SEM (n≥4); ns not significant; ***p < 0.001; *p<0.05. **(>F)** Measurement of PhIP-induced DNA double-strand breaks (DSB). Parental V79 and V79 CS cells were challenged with increasing PhIP concentrations for 24 h and DNA DSBs were determined by the neutral Comet assay. Data are presented as mean + SEM (n=4). ns: not significant; ***, p < 0.001.

Figure 3

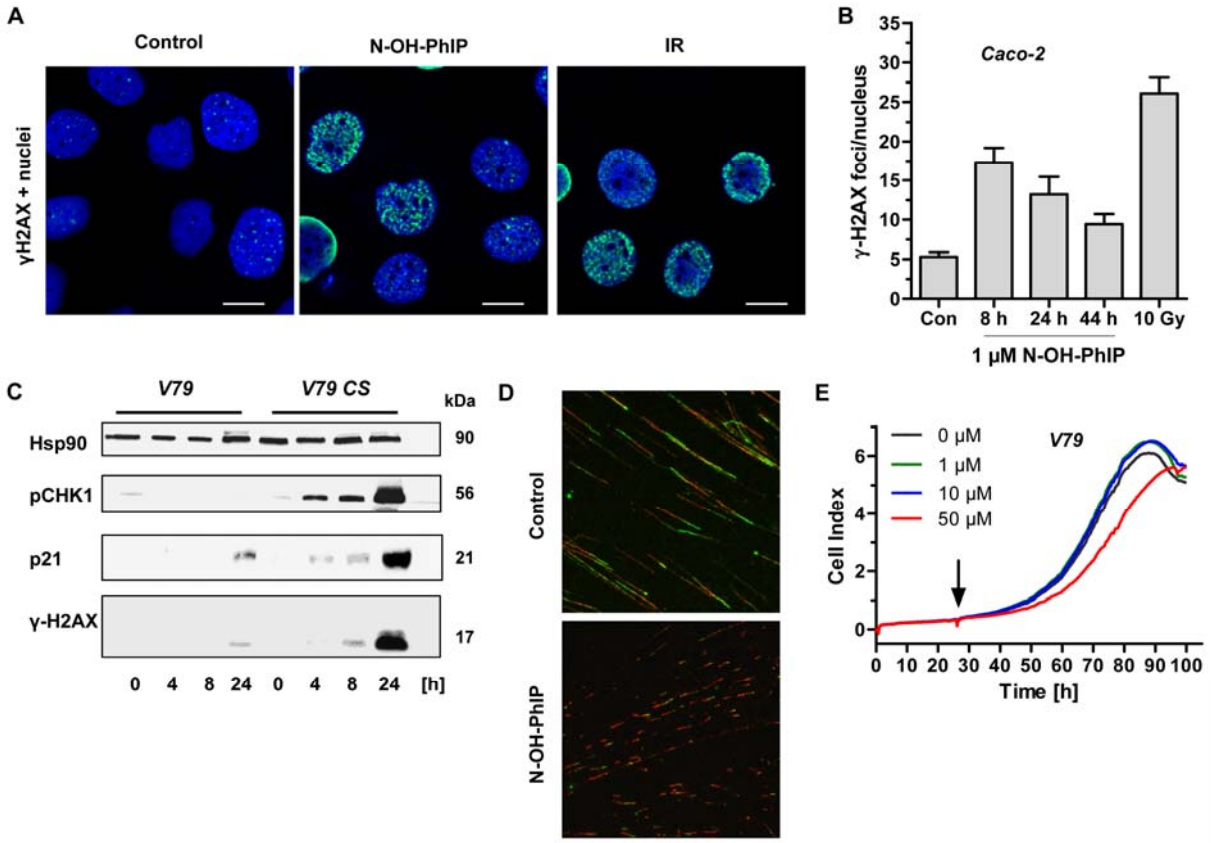

Figure 3: Analysis of γ-H2AX foci formation in Caco-2 cells and effects on cell growth in V79 cells. Detection of γ-H2AX foci in Caco-2 cells treated with 10 µM N-OH-PhIP for 8 h or irradiated with 10 Gy as positive control. Cells were then stained for γ-H2AX (green) and nuclei were counterstained with TO-PRO-3 (blue). Images were recorded by confocal microscopy. The scale bar represents 20 µm. **(B)** Cells were treated with 1 µM N-OH-PhIP for up to 44 h. As a positive control, cells were irradiated with 10 Gy. Cells were fixed and stained with a γ-H2AX antibody followed by an Alexa 488-coupled secondary antibody (green). Nuclei were counterstained with TO-PRO-3 (blue). Images were recorded by confocal microscopy and processed by ImageJ software. The number of γ-H2AX foci per nucleus were determined by ImageJ software and evaluated with GraphPad Prism 5.0 (> 100 cells per experiment). Data are expressed as mean + SEM. **(C)** Time-dependent DDR activation. Parental V79 and V79 CS cells were incubated with 50 µM PhIP and subjected to SDS-PAGE followed by Western blot analysis of p21, pCHK1 and γ-H2AX. Hsp90 served as loading control. **(D)** Overview images of DNA fiber assay in CaCO-2 cells, which were acquired by confocal microscopy **(E)** Effects of PhIP on parental V79 cells. Cells were treated with increasing concentrations of PhIP (black arrow) and growth was monitored for 72 h by performing an impedance-based analysis.

Figure 4

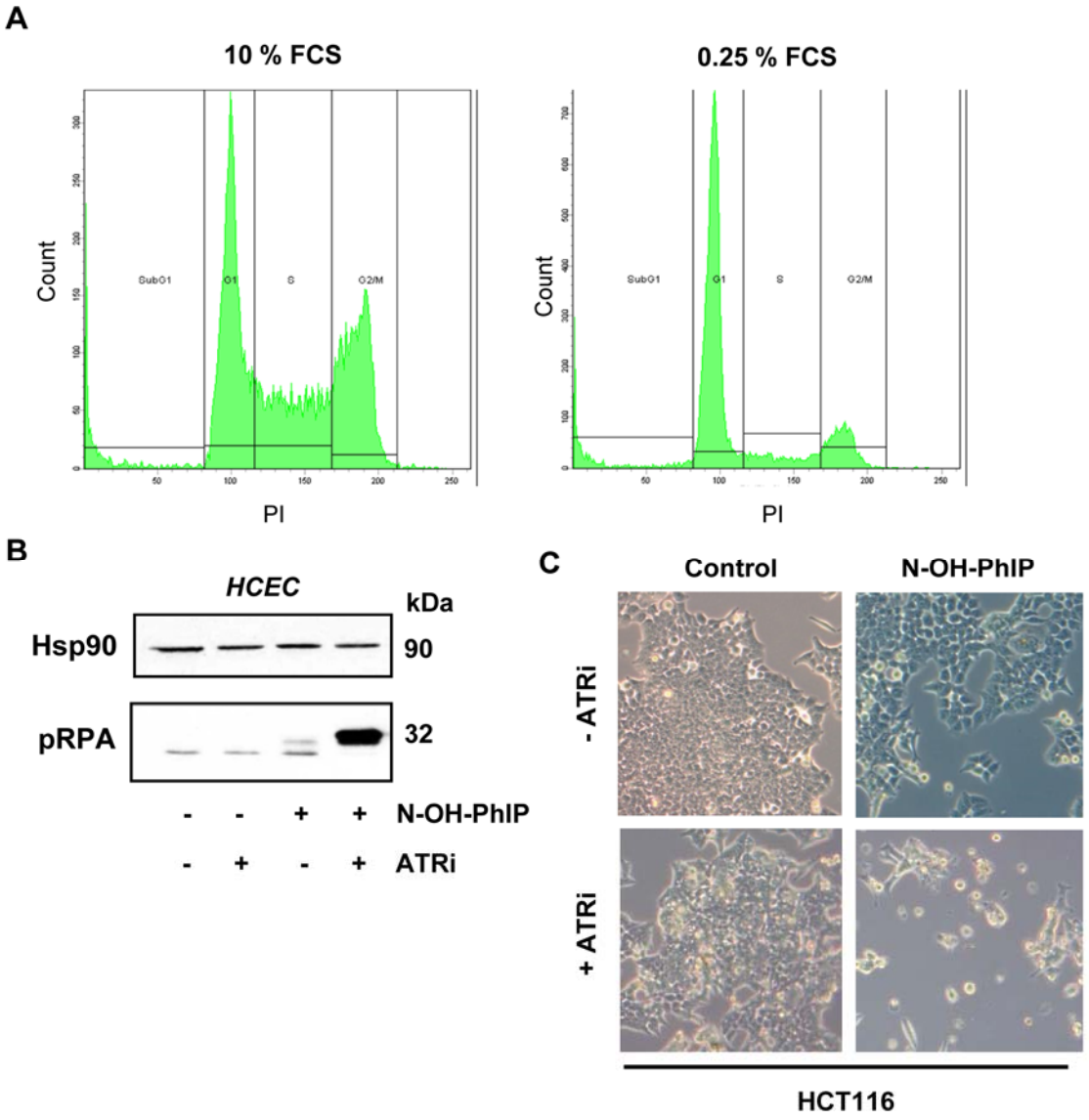

Figure 4: Analysis of cell cycle distribution and morphological changes in HCT116 cells upon N-OH-PhIP incubation. (A) Representative histograms of cell cycle distribution in HCT116 cells grown in normal medium (10% FCS) and in serum-deprived medium (0.25 % FCS) after 24 h. **(B)** Human colonic epithelial cells (HCEC) were treated with 10 µM N-OH-PhIP for 14 h. Samples were subjected to SDS-PAGE followed by Western blot analysis of pRPA and Hsp90, which served as loading control. **(C)** Effect of ATR inhibition on cell morphology. HCT116 cells were exposed to 2.5 µM N-OH-PhIP with or without ATR inhibitor for 48 h and morphology was monitored by phase-contrast microscopy.

Figure 5

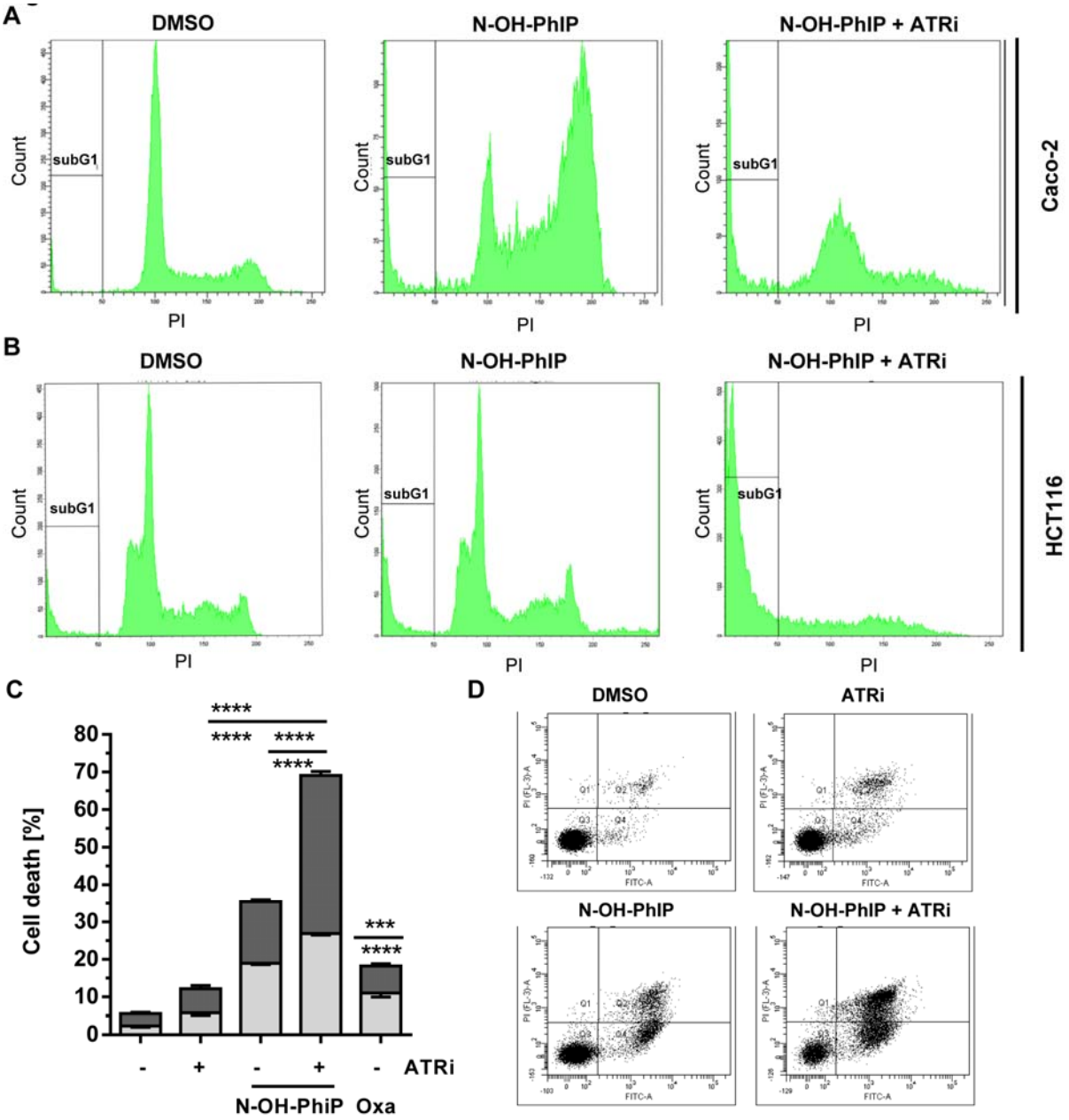

Figure 5: Effect of ATR inhibition on N-OH-PhIP-induce cell death in HCT116 and Caco-2 cells. **(A)** and **(B)** Effects of ATR inhibition on N-OH-PhIP-dependent cell death induction in Caco-2 and HCT116 cells. Cells were exposed to N-OH-PhIP with or without ATR inhibitor for 48 h. Cells were then processed as described and the subG1 population was determined by flow cytometry. Representative histograms are shown. **(C)** Annexin V/PI staining of HCT116 cells treated for 48 h with 5 µM N-OH-PhIP in the absence or presence of ATR inhibitor. Cells were processed as described in material & methods and analysed by flow cytometry. Bars in light grey represent early apoptotic cells (Annexin V-positive), while bars in dark grey represent late apoptotic/necrotic cells (Annexin V/PI-

double positive). Oxaliplatin (Oxa; 10 μM) was used as positive control. ****p<0.0001, ***p<0.001 (n≥3). **(D)** Representative histograms of HCT116 cells treated as indicated.